Asociación Argentina de Astronomía
BAAA, Vol. 52, 2009
J.J. Clariá, E. Brandi, A.E. Piatti & F.A. Bareilles, eds.

PRESENTACIÓN ORAL

Non-thermal radiation from galactic black hole coronae

F. L. Vieyro[1], G. E. Romero[1,2] & G. S. Vila[1]

(1) Instituto Argentino de Radioastronomía (IAR, CCT La Plata - CONICET)
(2) Facultad de Ciencias Astronómicas y Geofísicas - UNLP

Abstract. We study the effects of the injection of a non-thermal particle population in a two-temperature corona of hot plasma around an accreting black hole and we calculate the radiative output.

Resumen. Estudiamos los efectos de la inyección de una distribución de partículas no térmicas en la corona de un agujero negro acretante y calculamos la radiación de la misma.

1. Introduction

The detection of non-thermal radio, hard X-rays and gamma rays reveals that some Galactic compact objects are capable of accelerating particles up to very high energies. In order to explain the origin of the electromagnetic emission from this kind of sources we study the processes in a corona around an accreting black hole. We consider both electron and proton interactions with magnetic, photon and matter fields in the corona. Our calculations also include the radiation emitted by secondary particles (pions, muons and electron/positron pairs) in a self-consistent way. Finally, we take into account the effect of photon absorption, and compare a specific model with data obtained by the COMPTEL instrument from Cygnus X-1.

2. Basic scenario

The low-hard state of accreting black holes is characterized by the presence of a hot corona around the compact object. Figure 1 shows a scheme of the main components of the system. For this geometry, we assume a black hole of $M_{\rm BH} = 10 M_{\odot}$, a spherical corona with a radius $R_{\rm c} = 35 R_{\rm G}$ and an accretion disk that penetrates the corona up to a radius $R_{\rm d} < R_{\rm c}$. We suppose that the corona is homogeneous and in steady state.

We assume that the luminosity of the corona is 1% of the Eddington luminosity, which results in $L_{\rm c} = 1.3 \times 10^{37}$ erg s^{-1}.

The corona is composed of a two-temperature plasma, with an electron temperature $T_e = 10^9$ K and an ion temperature $T_i = 10^{12}$ K (e.g. Narayan & Yi 1994). By considering equipartition of energy, we can estimate the values of magnetic field and plasma density, which result in $B = 5.7 \times 10^5$ G and $n_i \sim n_e = 6.2 \times 10^{13}$ cm^{-3}, respectively.

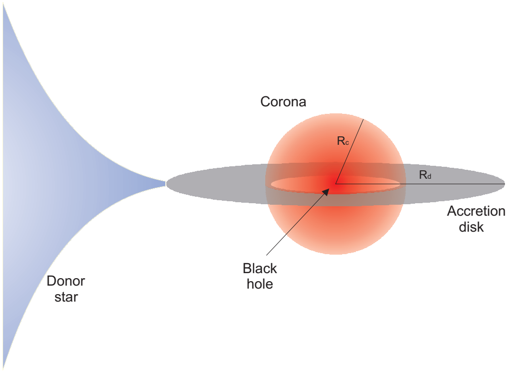

Figure 1. Schematic representation of the components of the system. (Not to scale)

The X-rays emission of the corona is characterized by a power law with an exponential cut-off at high energies,

$$n_{\rm ph}(E) = A_{\rm ph} E^{-\alpha} e^{-E/E_{\rm c}} {\rm erg}^{-1}\ {\rm cm}^{-3}. \tag{1}$$

According to the available information about Cygnus X-1 (e.g. Poutanen et al. 1997), we have adopted $\alpha = 1.6$ and $E_{\rm c} = 150$ keV.

3. Particle injection

The injection function for protons and electrons is a power-law in the energy of the particles $Q(E) = Q_0 E^{-\alpha} e^{-E/E_{\rm max}}$, as the consequence of diffusive particle acceleration by shock waves. Typically, $\alpha = 2.2$. The normalization constant Q_0 can be obtained from the total power injected in relativistic protons and electrons, $L_{\rm rel} = L_p + L_e$. This power $L_{\rm rel}$ was assumed to be a fraction of the luminosity of the corona, $L_{\rm rel} = \kappa L_{\rm c}$, with $\kappa = 10^{-2}$. The way in which energy is divided between hadrons and leptons is unknown, but different scenarios can be taken into account by setting $L_p = aL_e$. We consider models with $a = 100$ and $a = 1$.

4. Particle acceleration and losses

There are three processes of interaction of relativistic electrons and muons with magnetic, matter and photon fields in the corona and with the photon field of the disk: synchrotron radiation, inverse Compton scattering, and relativistic Bremsstrahlung. For protons and charged pions there are also three relevant processes: synchrotron radiation, proton-proton (or pion-proton) inelastic collisions and photohadronic interactions.

We consider two mechanisms of particle escape in the corona: advection and diffusion. In the case of advection, particles fall onto the compact object at a mean radial velocity $v = 0.1c$ (Begelman et al. 1990). In the case of diffusion, we consider that the corona is static and diffusion of the relativistic particles occurs in the Bohm regime.

The maximum energy that a relativistic particle can attain depends on the acceleration mechanism and the different processes of energy loss. The acceleration rate $t_{\rm acc}^{-1}$ for a particle of energy E in a magnetic field B is given by $t_{\rm acc}^{-1} = \frac{\eta ecB}{E}$, where $\eta \leq 1$ is a parameter that characterizes the efficiency of the acceleration. We have fixed $\eta = 10^{-2}$, which describes an efficient acceleration.

Figure 2 shows the cooling rates for different processes of energy loss, together with the acceleration and advection rates, for each type of particle. The main channel of energy loss for electrons is synchrotron radiation. For protons, both pp and $p\gamma$ interactions are relevant. However, in the model with advection, most protons fall into the black hole before radiating their energy.

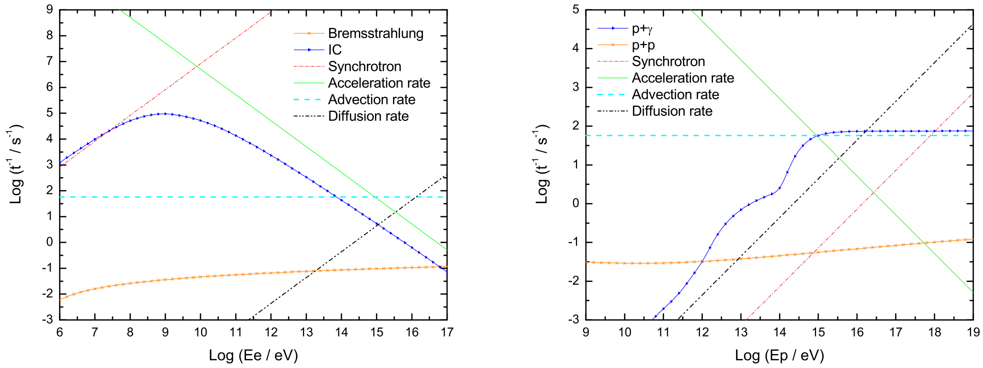

(a) Electron losses. (b) Proton losses.

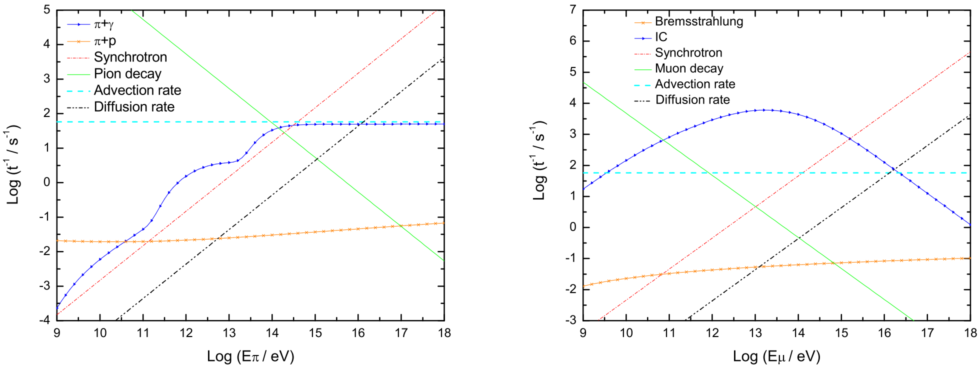

(c) Pion losses. (d) Muon losses.

Figure 2. Radiative losses in a corona under the physical conditions described.

The main channel of energy loss for pions is $\pi\gamma$ interaction, but an important fraction of pions decay before cooling. On the contrary, muons with energies above 10^{11} eV cool mostly by inverse Compton scattering.

5. Spectral energy distributions (SEDs)

In order to obtain the spectral energy distributions produced by the different radiative processes, we solve the transport equation for each kind of particle. To calculate the SEDs of different processes we have used Vila & Aharonian (2009) as reference. We also calculate the radiation emitted by secondary pairs, which are injected mainly by photon-photon annihilation.

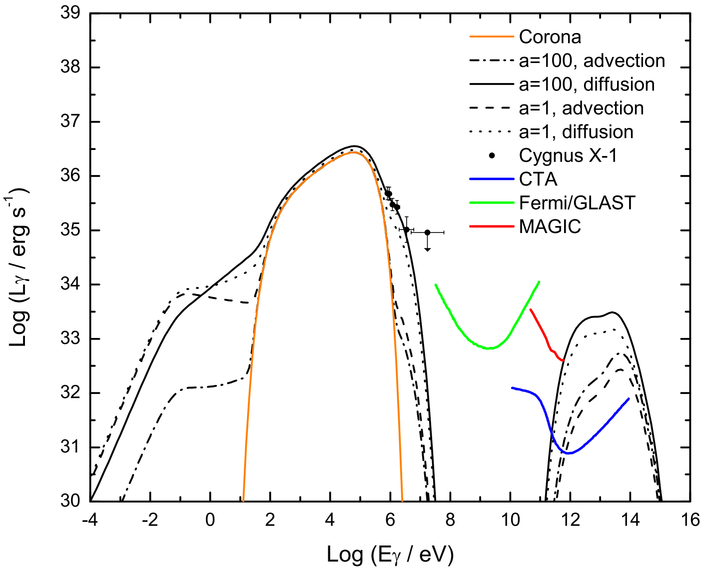

Figure 3. Spectral energy distributions. Observational data from COMPTEL of Cygnus X-1 (McConnell et. al. 2000)

Finally, we take into account the effects of photon-photon attenuation. The absorption can be quantified through the absorption coefficient or opacity τ. If the initial gamma-ray luminosity is $L_\gamma^0(E_\gamma)$, the attenuated luminosity $L_\gamma(E_\gamma)$ after the photon travels a distance l is $L_\gamma(E_\gamma) = L_\gamma^0(E_\gamma)e^{-\tau(l,E_\gamma)}$.

6. Results

Figure 3 shows the obtained luminosity for each set of parameters, the spectrum of Cygnus X-1 as observed by COMPTEL (McConnell et. al. 2000), and the sensitivity of different instruments that are able to detect the predicted emission.

It can be seen that the SED predicted by the model with an injection dominated by protons and diffusion agrees well with the observations of Cygnus X-1. In this case the radiative output is capable of reproducing the non-thermal tail detected by COMPTEL.

7. Acknowledgments

This research was supported by ANPCyT through grant PICT-2007-00848 BID 1728/OC-AR and by the Ministerio de Educación y Ciencia (Spain) under grant AYA 2007-68034-C03-01, FEDER funds.

References

Begelman M., Rudak B. & Sikora M. 1990, ApJ, 362, 38-51

McConnell M.L. et al. 2000, ApJ, 543, 928-937

Narayan R. & Yi I. 1994, ApJ, 428, L13

Poutanen J., Krolik J.H. & Ryde F. 1997, MNRAS, 292, L21-L25

Vila G.S. & Aharonian F.A. 2009, in: G.E. Romero & P. Benaglia (eds), *Compact Objects and their Emission*, AAA Book Series, Paideia, La Plata, p. 1-38